Published in IET Radar, Sonar and Navigation
Received on 23rd August 2010
Revised on 20th July 2011
doi: 10.1049/iet-rsn.2010.0262

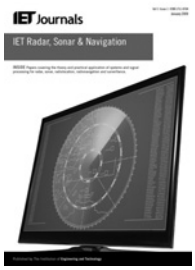

ISSN 1751-8784

Direction finding in frequency-modulated-based passive bistatic radar with a four-element Adcock antenna array

J. Wang H.-T. Wang Y. Zhao

National Laboratory of Radar Signal Processing, Xidian University, Xi'an, Shanxi 710071, People's Republic of China
E-mail: wangjun@xidian.edu.cn

Abstract: The Adcock antenna array is widely used in electronic warfare for direction finding of emitter sources. However, in frequency modulated (FM)-based passive bistatic radar (PBR) the traditional Adcock antenna-based direction finding methods cannot work well because weak target echoes are embedded in the background of strong direct signals, multipath and clutter echoes. A method using a four-element Adcock antenna array is developed for horizontal plane 360° target direction measurements for FM-based PBR. By using numerical simulations, the performance of the proposed method is studied for both single and multiple targets, and finally its effectiveness is demonstrated for real data.

1 Introduction

In recent years, the use of passive bistatic radar (PBR) for surveillance purposes has received renewed interests [1]. PBR systems exploit existing transmitters as illuminators of opportunity to perform target detection and localisation. Among the many different transmitters available and used in the past as sources of opportunity, the broadcast transmitters of the commercial radio stations in the frequency-modulated (FM) band 88–108 MHz are especially attractive – both for the generally high level of transmitted power and for the wide coverage [2, 3]. Especially in [2], using FM as a transmitter of opportunity, Howland showed that targets can be detected and tracked over a large area, at ranges of up to 150 km.

A target's direction of arrival (DOA) is very important for target location and tracking in PBR [2, 4]. Like the method presented in [2], we can first locate the target on a bistatic range ellipse using the target's relative bistatic range, and then locate the target on a certain point of that bistatic range ellipse using the target's DOA. We can also use the target's DOA and Doppler to locate and track it [4]. However, in PBR the weak target echoes are usually embedded in the background of direct signals, multipath and clutter echoes (DMC), and so conventional methods of direction finding (such as the method presented in [5]) cannot be used directly in PBR. So a different method of DOA estimation is needed in PBR.

Among the early researches, Howland used a pair of eight-element Yagi–Uda antennas to perform target bearing measurement [2, 4]. In [4], the receiving system was located far away from the transmitter source and mounted on a high tower, to decrease the DMC, and then spectral analysis was used to further decrease the influence of DMC on the target's DOA estimation; using this method, the influences of DMC are still very large, and there is directional ambiguity. In [2], DMC received by the two surveillance antennas was first cancelled, then, after delay-Doppler cross correlation between the remaining signals from the two antennas and direct signal, the estimation of target's DOA is performed using the phase difference of the correlated signals from the two antennas. Therefore in [2] the influences of DMC and noise on target's DOA estimation and the interference of targets are greatly decreased; however, there is still an element of directional ambiguity and the strong target may affect the DOA estimation of the weak target.

Owing to the advantage of omnidirectional coverage of the circular antenna array, many early works [6, 7] have referred to the application of the circular antenna array in PBR. However, they mainly considered using the circular antenna array to perform beamforming. In this paper, a method using a circular antenna array, a four-element Adcock antenna array, for target direction measurement in FM-based PBR is developed. Similar to [2], in this method DMC are also first cancelled, and then the estimation of target's DOA is performed using the phase difference of the correlated signals from the four elements of Adcock antenna array. However, because a four-element Adcock antenna array is used as surveillance antenna, a different target-DOA estimation method is developed; in our method, a strategy of solving quadrant ambiguity is applied to make certain that the target's DOA can be measured in the range of 360° in the horizontal plane. In addition, to decrease the influence of strong targets on the DOA estimation of weak targets, we point out that we can cancel the strong targets (while retaining in memory the DOA of strong targets) using the method presented in [8, 9], before measuring the DOA of weak targets.

Although we focus on the use of FM radio signal in this paper, it should be noted that the approach can be applied to many other transmissions of opportunity, such as waveform from digital modulation (DVB-T, DAB and GSM). Indeed, using digital waveforms as transmission of opportunity (which have better range resolution than FM), a better DOA estimation performance may be obtained.

2 Signal model

The geometry of the receiving system is shown schematically in Fig. 1. We use an independent antenna as reference antenna (which steered towards the FM transmitter) to receive the direct signal from the transmitter and the four elements of Adcock antenna array as the surveillance antennas which receive not only the direct signal but also the multipath, clutter echoes and the signals reflected from the moving target (it should be noted that we can also use only the four-element Adcock antenna array as both reference antenna and surveillance antenna, with the direct signal obtained by forming a beam in the direction of transmitter. In this paper we use an independent reference antenna to obtain a more clean direct signal). Then we transform the received analogue signals to digital baseband signals, respectively. Usually, the DMC received by the four elements of Adcock antenna array are much stronger than the signals reflected by the target. So we first remove DMC using the clutter cancellation algorithm, for example, batch version of extensive cancellation algorithm (ECA-B) [8]. As FM signal can be seen as a narrowband signal, after cancellation the signal from the four elements of Adcock antenna array can be represented as

$$s_{\mathrm{surv}_i}[n] = \sum_{m=1}^{N_\mathrm{T}} a_m d[n - \tau_m f_\mathrm{s}] \mathrm{e}^{\mathrm{j}2\pi f_{dm} n/f_\mathrm{s}} \mathrm{e}^{\mathrm{j}\phi_i} + z_{\mathrm{surv}_i}[n]$$
$$i = 1, 2, 3, 4 \quad n = 1, \ldots, N \tag{1}$$

where N is the total sample number and f_s is the sample rate; N_T is the number of target received by the four elements of Adcock antenna array; $i = 1, 2, 3, 4$ is the antenna element number; $d[n]$ is the nth sample of the direct signal (a delayed replica of the transmitted FM signal); a_m is the complex amplitude of the mth target; $\tau_m f_s$ is the delay bin (with respect to the direct signal) of the mth target; f_{dm} is the Doppler frequency of the mth target; $z_{\mathrm{surv}_i}[n]$ is the nth sample of the additive noise and remaining clutter of the ith array element ($i = 1, 2, 3, 4$); $\phi_i = \beta R \cos(\gamma_i - \varphi_m)$ is the phase difference of the ith array element with respect to the centre of antenna array, φ_m is DOA of the mth target and $\gamma_i = \pi(i-1)/2$ is the angle of the nth element, $\beta = 2\pi/\lambda$ (λ is the wavelength) and R is the radius of the antenna array (as depicted in Fig. 2.).

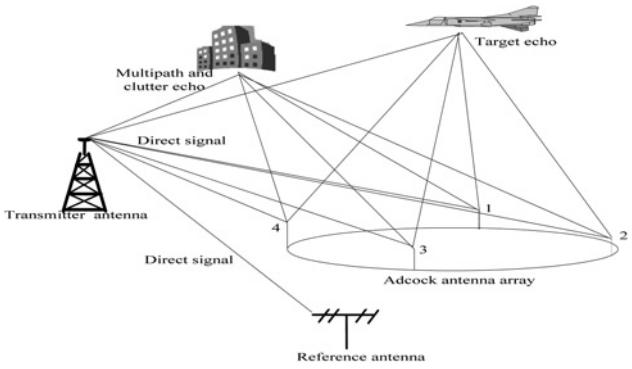

Fig. 1 *Receiving geometry of the direction finding system*

The signal received by the reference antenna can be represented as

$$s_{\mathrm{ref}}[n] = A_{\mathrm{ref}} d[n] + z_{\mathrm{ref}}[n] \quad n = 1, \ldots, N \tag{2}$$

where A_{ref} is the complex amplitude and $z_{\mathrm{ref}}(n)$ is additive noise.

In order to improve the signal − noise ratio (SNR) of targets and further decrease the influence of remaining DMC on target DOA estimation and the mutual interference of targets, we evaluate the delay-Doppler cross-correlation function between the remaining signals from each array element and the reference signal, respectively

$$\xi[i, l, p] = \sum_{n=0}^{N-1} s_{\mathrm{surv}_i}[n] s^*_{\mathrm{ref}}[n - l] \mathrm{e}^{-\mathrm{j}2\pi pn/N} \tag{3}$$

where l is the time bin representing the time delay $\tau[l] = l/f_s$, p is the Doppler bin representing the Doppler frequency $f_d = pf_s/N$, $*$ represents conjugate.

The value of the ith cross-correlation function in the Doppler bin and time bin of the first target ($l_1 = \tau_1 f_s$, $p_1 = f_{d1} N/f_s$) can be represented as

$$\xi[i, l_1, p_1] = \xi_t[i, l_1, p_1] + \xi_s[i, l_1, p_1] + \xi_n[i, l_1, p_1] \tag{4}$$

where $\xi_t(i)$ is the peak caused by the first target and can be written as

$$\xi_t[i, l_1, p_1] = \sum_{n=0}^{N-1} A_{\mathrm{ref}} a_1 d[n - \tau_1 f_s] d^*[n - \tau_1 f_s] \mathrm{e}^{\mathrm{j}\beta R \cos(\varphi_i - \varphi_1)} \tag{5}$$

$\xi_s(i)$ is the total side lobe of other targets and can be written as

$$\xi_s[i, l_1, p_1] = \sum_{n=0}^{N-1} \sum_{m=2}^{N_\mathrm{T}} A_{\mathrm{ref}} a_m d[n - \tau_m f_\mathrm{s}]\, d^*[n - \tau_1 f_\mathrm{s}] \chi_{i,m} \tag{6}$$

With $\chi_{i,m} = \mathrm{e}^{\mathrm{j}2\pi(f_{dm} - f_{d1})n/f_s} \mathrm{e}^{\mathrm{j}\beta R \cos(\varphi_i - \varphi_m)}$, $\xi_n(i)$ is the disturbance

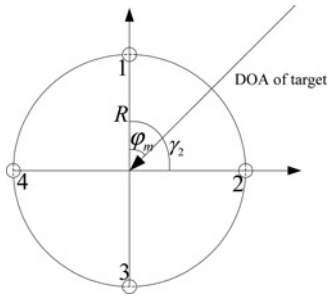

Fig. 2 *Adcock antenna array geometry*

doi: 10.1049/iet-rsn.2010.0262

and can be written as

$$\xi_n[i, l_1, p_1] = \sum_{n=0}^{N-1} (s_{\text{surv}_i}[n] z^*_{\text{ref}}[n - \tau_1 f_s] + z_{\text{surv}_i}[n] s_{\text{ref}}[n - \tau_1 f_s]) e^{-j2\pi f_{d1} n/f_s} \quad (7)$$

3 Direction finding

In this section, we will give a method to find DOA of targets. First we consider the condition of single target and then multiple targets.

3.1 Single target

When only one target is considered, the disturbance term $\xi_n(i)$ is set to be zero for convenience. So (4) can be rewritten as

$$\xi[i, l_1, p_1] = \xi_t[i] \quad (8)$$

According to (5), (8) and $\gamma_i = \pi(i-1)/2$, we can rewrite the values of the four cross-correlation functions as

$$\begin{aligned} D1 &= \xi[1, l_1, p_1] \cong A e^{j\theta} e^{j\beta R \cos(\varphi_1)} \\ D2 &= \xi[2, l_1, p_1] \cong A e^{j\theta} e^{j\beta R \sin(\varphi_1)} \\ D3 &= \xi[3, l_1, p_1] \cong A e^{j\theta} e^{-j\beta R \cos(\varphi_1)} \\ D4 &= \xi[4, l_1, p_1] \cong A e^{j\theta} e^{-j\beta R \sin(\varphi_1)} \end{aligned} \quad (9)$$

where

$$A = \text{amplitude}\left(\sum_{n=1}^{N} A_{\text{ref}} a_1 d(n - \tau_1 f_s) d^*(n - \tau_1 f_s)\right) \quad (10)$$

and

$$\theta = \text{angle}\left(\sum_{n=1}^{N} A_{\text{ref}} a_1 d(n - \tau_1 f_s) d^*(n - \tau_1 f_s)\right) \quad (11)$$

Then we can acquire the following equations

$$\begin{aligned} X_{13} &= |D1/|D1| - D3/|D3|| = 2|\sin(\beta R \cos(\varphi_1))| \\ X_{24} &= |D2/|D2| - D4/|D4|| = 2|\sin(\beta R \sin(\varphi_1))| \end{aligned} \quad (12)$$

If R and λ have the relation $R \le \lambda/4$, the inequality (13) holds for any φ_1

$$\begin{aligned} -\frac{\pi}{2} \le \beta R \cos(\varphi_1) \le \frac{\pi}{2} \\ -\frac{\pi}{2} \le \beta R \sin(\varphi_1) \le \frac{\pi}{2} \end{aligned} \quad (13)$$

Therefore in this case the arcsine of $X_{13}/2$ and $X_{24}/2$ can be written as

$$\begin{aligned} \arcsin(X_{13}/2) &= \beta R |\cos(\varphi_1)| \\ \arcsin(X_{24}/2) &= \beta R |\sin(\varphi_1)| \end{aligned} \quad (14)$$

Then we can acquire

$$\hat{\varphi}_1 = \arctan \frac{|\arcsin(X_{24}/2)|}{|\arcsin(X_{13}/2)|} \quad (15)$$

So far, there is the remaining problem of placing $\hat{\varphi}_1$ in the proper quadrant. This requires the knowledge of the sign of $\cos(\varphi_1)$ and $\sin(\varphi_1)$.

Consider the difference between $D1$ and $D3$, and the summation of $D1$ and $D3$

$$\begin{aligned} D1 - D3 &= j2A e^{j\theta} \sin(\beta R \cos(\varphi_1)) \\ D1 + D3 &= 2A e^{j\theta} \cos(\beta R \cos(\varphi_1)) \end{aligned} \quad (16)$$

Then we multiply the image part of $D1 - D3$ with real part of $D1 + D3$

$$\begin{aligned} &\text{Im}\{D1 - D3\}\text{Re}\{D1 + D3\} \\ &\quad = 4A^2 \cos^2(\theta) \sin(\beta R \cos(\varphi_1)) \cos(\beta R \cos(\varphi_1)) \end{aligned} \quad (17)$$

According to (13) and (17), we can obtain the formulation (18)

$$\text{sign}(\cos(\varphi_1)) = \text{sign}(\text{Im}\{D1 - D3\}\text{Re}\{D1 + D3\}) \quad (18)$$

The sign of $\sin(\varphi_1)$ can be acquired as the same

$$\text{sign}(\sin(\varphi_1)) = \text{sign}(\text{Im}\{D2 - D4\}\text{Re}\{D2 + D4\}) \quad (19)$$

It should be noted that in this section the results are acquired in the absence of disturbance, and so the estimation result of the target's DOA is exact. However, in practice the disturbance always exists, which will induce estimation error.

3.2 Multiple targets

In this section, the case of multiple targets is considered. The FM radio signal has a characteristic of noise-like. In the ambiguity function of FM signal, the side lobe outside the main lobe is usually low. So after delay-Doppler cross correlation, when two targets are not very close, the interference of the two targets is similar to the influence of noise or clutter on targets. However, in this paper, we cannot give the strict boundary with regard to when the two targets are separated adequately, because in FM-based PBR, the side lobe structure is a time-varying feature which changes with the programme being broadcast and total coherent integration time. Fortunately, in PBR the total coherent integration time is usually long, which can bring a high-enough Doppler resolution. For example, when the total coherent integration time is 0.4 s, the Doppler resolution is calculated as 2.5 Hz ($\Delta f = 1/T$, Δf is the Doppler resolution, T is the total coherent integration time). As a result, most targets can be separated in the Doppler domain, although the poor range resolution (typically 3–30 km) of FM-based PBR induces that some targets cannot be separated in the range domain. Therefore when multiple targets (and all of them are separated in the range or Doppler domain) received by the four elements of Adcock antenna array and the energy of all targets are similar (i.e. no strong targets exist), the DOA of all targets can be measured using the method described above. If strong targets exist, we can first evaluate the DOA of strong

Table 1 Related parameters for both simulated and real data

radius of the array R	0.6 m
wavelength λ	3.22 m
total number of samples N	100 000
sample frequency f_s	250 kHz

targets, and then remove the strong targets. References [8, 9] presented their own method regarding how to remove the strong targets. In this paper we use the method in [8], that is, the strong targets can be cancelled using the formulation (20)

$$\boldsymbol{s}_{\text{surv1}_i} = [\boldsymbol{I}_N - \boldsymbol{X}(\boldsymbol{X}^{\text{H}}\boldsymbol{X})^{-1}\boldsymbol{X}^{\text{H}}]\boldsymbol{s}_{\text{surv}_i} \quad i = 1, 2, 3, 4 \qquad (20)$$

where $\boldsymbol{s}_{\text{surv}_i} = [s_{\text{surv}_i}[1], \ldots, s_{\text{surv}_i}[N]]$ represents the signal vector (where the DMC has been cancelled) from the ith array element; $\boldsymbol{I}_N$ is an $N \times N$ identity matrix, H represents conjugate transpose; $\boldsymbol{X}$ is a time-delayed and frequency-shifted replica of the reference signal, which defines the subspace spanned by the strong target. With the respect to the exact expression of $\boldsymbol{X}$, the readers can refer to [8].

After removing the strong target, the DOA of other targets can be measured.

4 Performance analyses

In this section, we will give some simulated and real data analysis. The related parameters for both simulated and real data are described in Table 1. From Table 1 we can easily know that the condition $R \leq \lambda/4$ is met. It should be noted that ECA-B [8] is used to cancel the DMC.

4.1 Results based on simulated data

The direct signals $d[n]$ used in the simulation are taken as the FM signals collected in the actual environment by a directional antenna with 3 dB beamwidth of about 40°. Multipath and target echoes are simulated as time-delayed or frequency-shifted replicas of these direct signals with amplitude modulated.

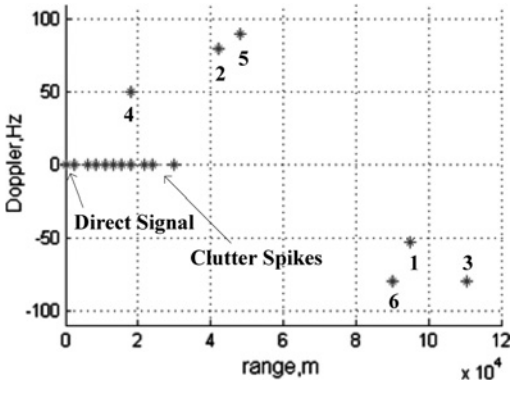

Fig. 3 *Sketch of reference scenario*

An example of the range-Doppler domain considered in this section is illustrated schematically in Fig. 3. It includes the direct signal with a direct SNR of about 35 dB and the number of scatters $N_c = 10$. Clutter spikes can be observed with a clutter-to-noise ratio in the range of 5–30 dB in range bins between 0 and 30 km. There are six target echoes whose characteristics are listed in Table 2. Note that target 1 is labelled as 'strong target' since its SNR is well above those of 2–6. The SNR on the reference antenna is 40 dB. It should be noted the SNR in this section is calculated before delay-Doppler cross correlation.

First, we consider only the echo of target 2 received by the four elements of Adcock antenna array, that is, the echoes of other targets in Fig. 3 are not received, but the direct signal and clutters are still retained as depicted in Fig. 3. The SNR of target 2 is set at different values. Then the DOA of target 2 is measured using the method described above.

With respect to each SNR of target 2, 100 independent trials have been conducted to give the root mean-square error (RMSE) of the estimation

$$\text{RMSE} = \left[\sum_{n=1}^{100}(\hat{\varphi}(n) - \varphi)^2/100\right]^{1/2} \qquad (21)$$

where $\hat{\varphi}(n)$ is the estimation of the nth trial. The results in Fig. 4 show that the RMSE is about 4° when the SNR is equal to about −33 dB, and is about 0.7° when the SNR is equal to about −20 dB. This estimation accuracy can be considered high when the weak target is embedded in the background of strong DMC and noise.

Then all the targets depicted in Fig. 3 and Table 2 are considered to be received by the four elements of the Adcock antenna array. In this case, first we cancel the DMC, then after delay-Doppler cross correlation between the signals from each array element and the reference signal; each target's DOA is measured using the method described in Section 3.1. In order to decrease the influence

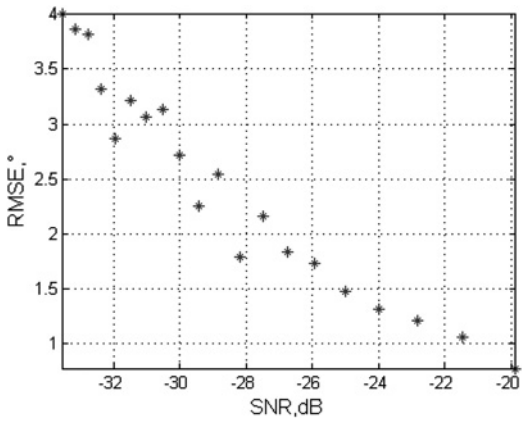

Fig. 4 *Performance of DOA estimation in the case of one target, bearing 138.6°*

Table 2 Target echoes parameters for simulated scenarios

Target	1	2	3	4	5	6
range, km	94.8	42	110.4	18	48	90
Doppler frequency, Hz	−53	80	−80	50	90	−80
SNR, dB	−3.5	−20	−21.6	−21.6	−20	−18.7

doi: 10.1049/iet-rsn.2010.0262

of target 1 on other targets' DOA estimation, we then remove target 1 using the formulation (20).

Then after delay-Doppler cross correlation between $\boldsymbol{s}_{\mathrm{surv1_i}}$ and the reference signal, the DOA of target 2–6 can also be measured. The results before and after cancelling the first target are shown in Tables 3 and 4 (100 independent trials have been conducted). From Table 3 we can see that when the strong target exists, the DOA estimation accuracy of targets close to the strong target is poor (such as target 3 and 6, especially, target 6. It should be noted there are 11 trials where target 3 is located in a wrong quadrant, that is, we acquired the wrong sign of $\cos(\varphi_3)$ or $\sin(\varphi_3)$. These 11 trials have been eliminated when we calculate the RMSE and mean of target 3 in Table 3.). However, the influence of strong target on targets far away is much smaller (such as target 2, 4 and 5). From Table 4 we can see that when no strong target exists the influence of one target on another is small.

Finally, in order to show the interference of two targets in more detail, we consider another case that the four elements of Adcock antenna array receive only two pure target echoes with the same energy, that is, no DMC and additive noise are included. We fix the first target echo in the bistatic range of 0 m and the Doppler frequency of 0 Hz, whereas the second target echoes are set to be in the different bistatic range and Doppler frequency. Then after delay-Doppler cross correlation between the received signal and direct signal, the DOA of the second target is estimated.

Table 3 Targets' DOA estimation performance before cancelling the strong target

Target	1	2	3	4	5	6
true DOA, °	253.8	138.6	183.6	282.6	192.6	12.6
mean of estimation, °	253.8	138.0	179.7	281.6	191.6	253.9
RMSE, °	0.1258	1.0517	4.2621	1.3786	1.4030	241.2667

Table 4 Targets' DOA estimation performance after cancelling the strong target

Target	2	3	4	5	6
true DOA, °	138.6	183.6	282.6	192.6	12.6
mean of estimation, °	137.9	184.6	281.8	192.8	12.9
RMSE, °	1.1037	1.4640	1.2476	0.9568	0.7784

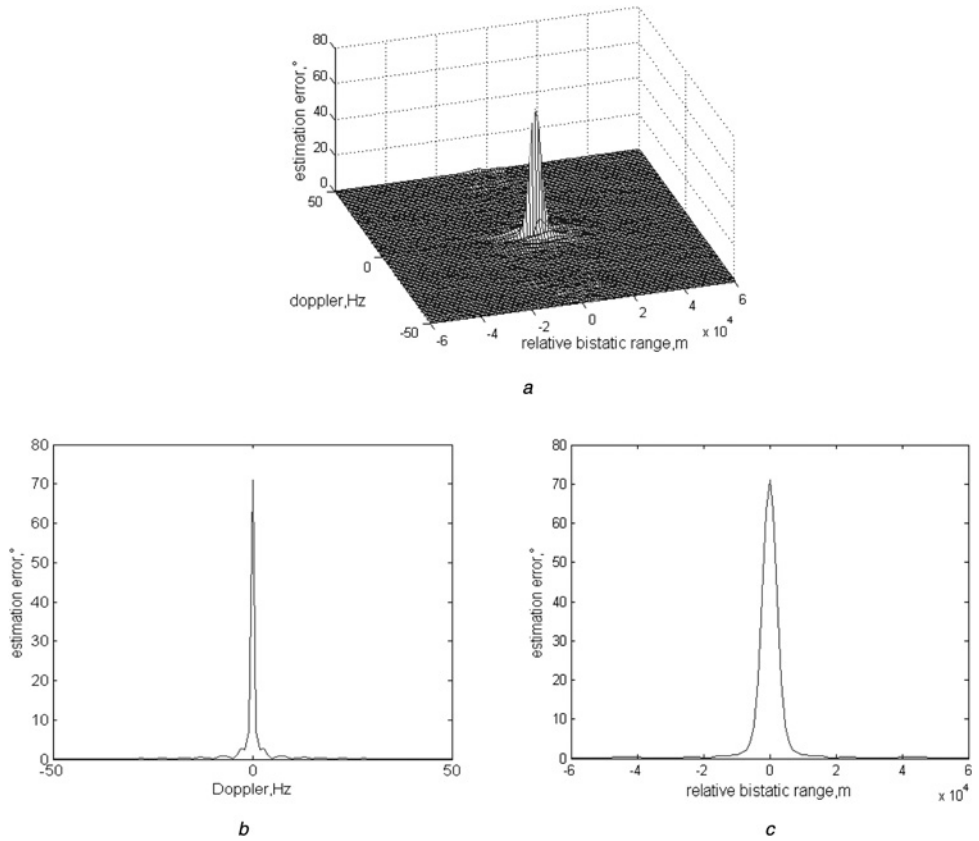

Fig. 5 *DOA estimation errors of the second target when it locates in a different bistatic range and Doppler frequency*

a 2D representation
b Zero range cut
c Zero Doppler cut

The DOA estimation errors (the difference between the actual value and estimated value) of the second target when it locates in the different bistatic range and Doppler frequency are shown in Fig. 5. It should be noted that in this simulation the actual bandwidth of the direct signal is 100 kHz corresponding to the bistatic range resolution of 3 km, the total integration time is 0.4 s (100 000 sample) corresponding to the Doppler resolution of 2.5 Hz. The actual DOA of the two targets is 338 and 122°, respectively. From Fig. 5 we can see that when the second target is within the main lobe of the first target, the interference of the two targets are very large, which induces the DOA estimation error to reach up to 10°. However, when the second target locates outside the mainlobe of the first target, the DOA estimation errors is usually less than 2°. The further the two targets separate, the less the interference of the two targets tends to be. For example, when the second target locates in the range of 4800 m and Doppler frequency of 4 Hz, the DOA estimation error is 1.5°, whereas the DOA estimation error is 0.6° when the second target locates in the range of 7200 m and Doppler frequency of −8 Hz.

4.2 Results based on real data

In this section the effectiveness of the above method are demonstrated using a real data set derived from an experimental PBR. In this design, two antennas (one is the reference antenna with 3 dB beamwidth of about 40° pointing towards an FM transmitter, and the other is the Adcock antenna array) are used to exploit FM signals. Outputs from the antennas are then connected to a high-quality five-channel A/D converter with a 14-bit resolution. After sample, the digital signals are transferred to PC in order to be processed by MATLAB. The processing flow diagram in MATLAB is shown in Fig. 6. As seen in Fig. 6, after digital down-conversion to a complex baseband, appropriate filtering and channel phase calibration, the signals were used to detect targets. In this paper a point in the range-Doppler surface can be seen as a target echo only when its amplitude is 8 dB above the average power level of the total range-Doppler surface and such points can be detected in consecutive range-Doppler surface for the same or adjacent cells. In the end, we find DOA of the detected targets using the method described above. The phase mismatch between the four surveillance channels is removed in software using a simple calibration coefficient. The experimental data were recorded during a field experiment in the northwest part of china near a civil airport.

Fig. 7 represents a target DOA estimation result when only one target is received by the four elements of the Adcock antenna array. In Fig. 7 the value of DOA being equal to 0° means that the target has not been detected at that time. However, compared with the simulations, the real data may be exposed to the worse remaining DMC and pollution of reference signal, as well as the remaining phase mismatch of surveillance channels. This brings out the fact that the DOA estimation error of real data may be larger than that of simulated data (in this paper we cannot give the RMSE of DOA estimation of real data because the true location of the non-cooperative target is not known to us). From Fig. 7 we can see that the values of the measured DOA are consecutive. Using the target's relative bistatic range and DOA, we can determine the location of the target. This result is shown in Fig. 8 where *Rx* represents receiver and *Tx* represents transmitter.

Fig. 9 represents the DOA estimation result when two targets are received by the four elements of Adcock antenna array. Although the relative bistatic range (about 20–50 km) of target 1 is higher than that (about 70–100 km) of target 2, the echo energies of these two targets are similar (this may be because the radar cross-section (RCS) of target 1 is smaller than that of target 2). So the DOA estimation of these two targets are performed in the same range-Doppler surface, that is, no target is removed when the DOA of the other target is measured. As seen in Fig. 9, both targets 1 and 2 can be seen as being located in the direction of

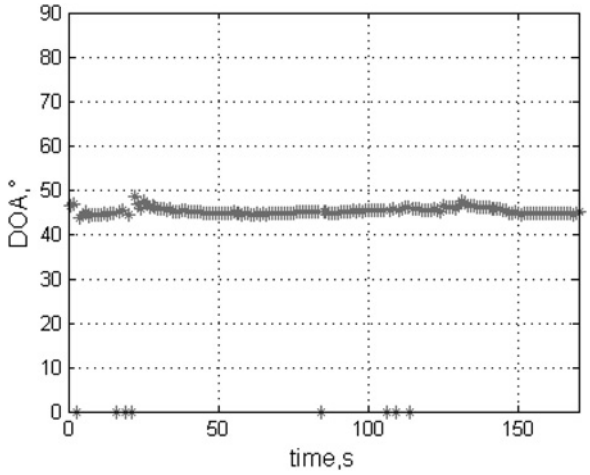

Fig. 7 *DOA estimation result when one target is received*

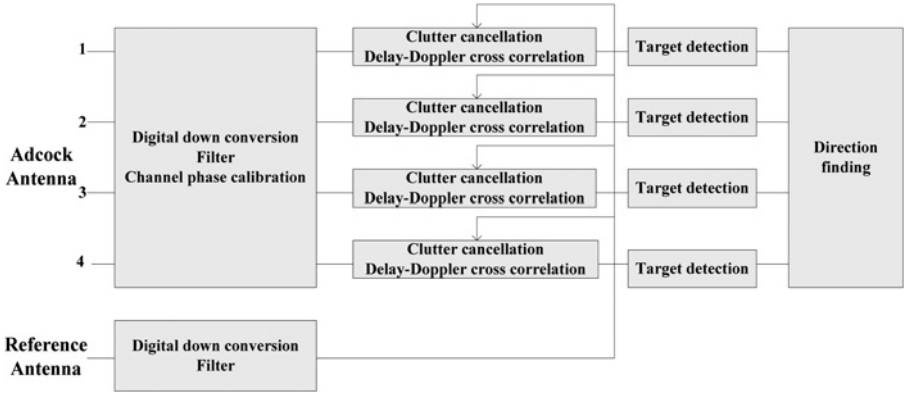

Fig. 6 *Processing flow diagram in MATLAB*

doi: 10.1049/iet-rsn.2010.0262

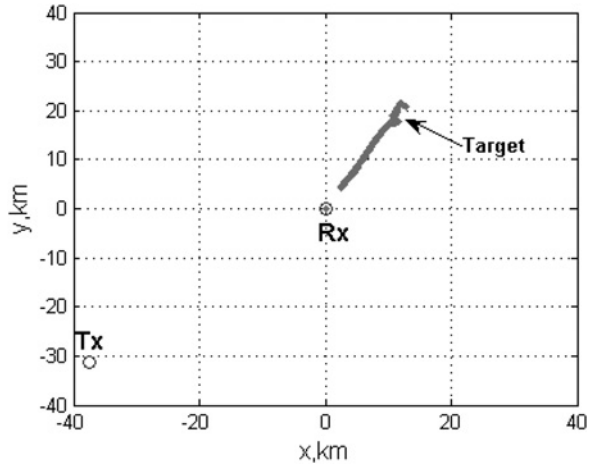

Fig. 8 *Target track when one target is received*

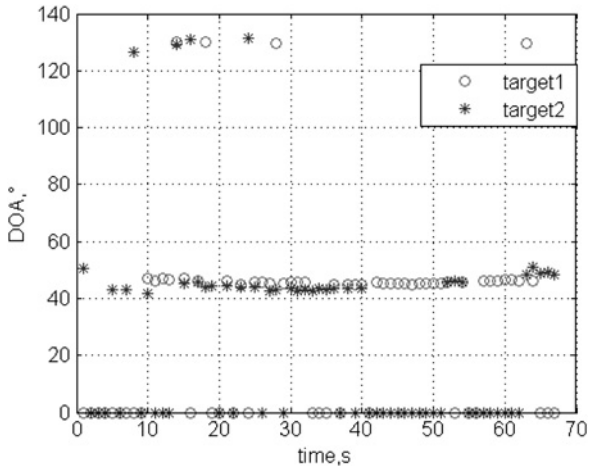

Fig. 9 *DOA estimation result when two targets are received*

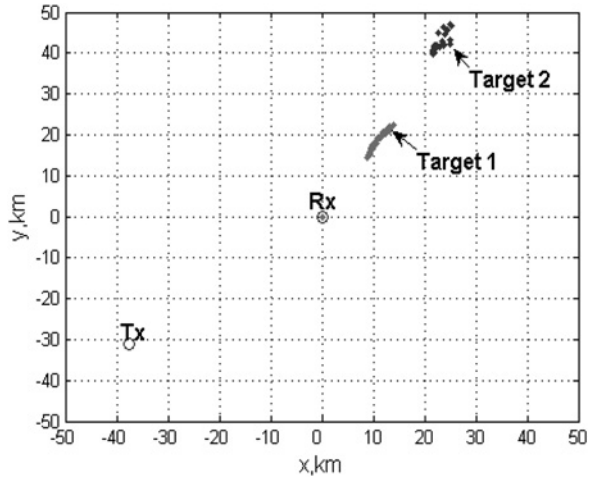

Fig. 10 *Target tracks when two targets are received*

about 45°. However, there are some detections whose DOA are about 130°. The reason causing this is that we locate these detections in a wrong quadrant. After adjusting these detections in an accurate quadrant, the tracks of targets 1 and 2 are shown in Fig. 10.

5 Conclusions

This paper develops a method of direction finding in FM-based PBR with a four-element Adcock antenna array. In this method, we first cancel DMC, and then if there are strong targets, the strong targets are removed after the DOA estimation of the strong targets is performed. So we eliminate not only the influence of DMC on the target DOA measurement but also the influence of strong targets on the weak targets. Simulated results show that the estimation accuracy is high in the case of different SNR when a single target is considered. When multiple targets have been considered, the high estimation accuracy can also be acquired in the case of no strong targets (or the strong targets have been removed). This method can measure the target's DOA in the range of 360° in the horizontal plane. Finally, its effectiveness is demonstrated with the application to real data.

In this paper, all the real-life targets reported are located on the extended baseline. In this geometry, aspects such as range resolution and Doppler resolution are roughly like that in the monostatic case, that is, the bistatic angle is close to zero. However, in reality, the transmitter–receiver-targets geometry can be random. When the system geometry configuration is different, a different DOA estimation performance may be obtained. So in the future work, the DOA estimation performance with transmitter–receiver-targets in other geometry should be validated.

6 Acknowledgments

The authors would like to thank the anonymous reviewers and the associate editor for their valuable comments and suggestions that improved the clarity of this manuscript. This work is supported by the National Natural Science Foundation of China (60472087) and Program for Changjiang Scholars and Innovative Research Team in University (IRT0954).

7 References

1 Howland, P.E.: 'Special issue on passive radar systems', *IEE Proc. Radar Sonar Navig.*, 2005, **152**, (3), pp. 106–223
2 Howland, P.E., Maksimimuk, D., Reitsma, G.: 'FM radio based bistatic radar', *IEE Proc. Radar Sonar Navig.*, 2005, **152**, (3), pp. 107–115
3 Baker, C.J., Griffiths, H.D., Papoutsis, I.: 'Passive coherent location radar systems – part 2: waveform properties', *IEE Proc. Radar Sonar Navig.*, 2005, **152**, (3), pp. 160–168
4 Howland, P.E.: 'Target tracking using television-based bistatic radar', *IEE Proc. Radar Sonar Navig.*, 1999, **146**, (3), pp. 166–174
5 Chan, Y.T., Lee, B.H., Inkol, R., Yuan, Q.: 'Direction finding with a four-element Adcock-butler matrix antenna array', *IEEE Trans. Aerosp. Electron. Syst.*, 2001, **34**, (4), pp. 1155–1162
6 Malanowski, M., Kulpa, K.S.: 'Digital beamforming for passive coherent location radar'. IEEE Radar Conf., Rome, Italy, 2008
7 Tsai, P.-H.E., Ebrahim, K., Lange, G., Paichard, Y., Inggs, M.: 'Null placement in a circular antenna array for passive coherent location systems'. IEEE Radar Conf., Washington, DC, USA, 2010
8 Colone, F., O'hagan, D.W., Lombardo, P., Baker, C.J.: 'A multistage processing algorithm for disturbance removal and target detection in passive bistatic radar', *IEEE Trans. Aerosp. Electron. Syst.*, 2009, **45**, (2), pp. 698–722
9 Kulpa, K.S., Czekala, Z.: 'Masking effect and its removal in PCL radar', *IEE Proc. Radar Sonar Navig.*, 2005, **152**, (3), pp. 174–178